Deep Learning in Healthcare: Technical Insights and Neural Network Applications in Medical Diagnosis and Prognosis

Dhruv Garg

Abstract

The integration of Deep Learning (DL) into healthcare has fundamentally transformed the landscape of medical diagnosis and prognosis, offering capabilities that surpass traditional methodologies. This paper provides a comprehensive technical evaluation of neural network architectures—including Convolutional Neural Networks (CNNs), Recurrent Neural Networks (RNNs), and Transformers—analyzing their specific applications in medical imaging, Electronic Health Record (EHR) analysis, and genomics. Key case studies are examined, such as CheXNet for pneumonia detection and Google's Lymph Node Assistant (LYNA), which achieved 99% accuracy in identifying metastatic breast cancer, demonstrating the superior sensitivity and specificity of these models compared to unassisted human diagnosis. However, despite these advancements, significant barriers to clinical adoption remain, including data scarcity, privacy regulations like HIPAA, and the "black box" interpretability problem. The study consequently explores advanced methodologies such as Explainable AI (XAI) and Graph Neural Networks (GNN) as solutions to these challenges, concluding that sustainable integration requires robust measures for transparency, data privacy, and interdisciplinary collaboration.

Keywords: Deep Learning, Artificial Intelligence, Medical Imaging, Neural Networks, Electronic Health Records (EHR), Convolutional Neural Networks (CNN), Explainable AI (XAI), Medical Diagnosis, Prognosis.

1. INTRODUCTION

1.1 Brief History of AI in Medicine

In 1950, Alan Turing, a British mathematician and computer scientist, also known as the father of theoretical computer science, published a paper titled “Computing Machinery and Intelligence”. In the paper, Turing talks about the possibility of creating machines that think [1]. He devised a famous Turing test: If a machine could execute a conversation that was indistinguishable from a conversation with a human being, then it was reasonable to say that the machine was "thinking" [2]. Five years later, John McCarthy coined the term “Artificial Intelligence” in a workshop proposal titled “A Proposal for the Dartmouth Summer Research Project on Artificial Intelligence.” Later in 1956, the field of artificial intelligence was officially established.

The use of AI in Medicine began in the 1970s with the development of “expert systems.” Amongst the earliest of these systems was MYCIN, developed at Stanford University to diagnose bacterial infections and recommend antibiotic treatments. It used a rule-based system with around 500 production rules to analyze patient symptoms and lab results. However, due to ethical considerations, MYCIN was never implemented in clinical practice [3]. Another pioneering medical AI was INTERNIST-I, which was designed to assist with diagnosis in internal medicine. This project was developed at the University of Pittsburgh, but it was not dependable enough for clinical use due to limitations like the inability to reason.

The 1980s and 1990s served as a transitional period. The proliferation of AI research, marked by the formation of the American Association for Artificial Intelligence in 1979, led to advancements that laid the groundwork for the data-centric future. However, the field experienced limited progress until the advent of deep learning in the 2010s. The implementation of Convolutional Neural Network (CNN) in medical imaging showed significant promise in specific diagnostic tasks [4]. In 2012, AlexNet, a convolutional neural network (CNN) architecture, revolutionized the field of deep learning for image recognition. This triggered the adoption of deep learning across medical domains [5].

Recent years have witnessed significant growth in AI-based healthcare applications. The availability of large-scale medical datasets, advances in computational power, and breakthroughs in neural network architecture are key factors for this growth [6].

1.2 Importance of deep learning in modern healthcare

Deep learning is a subset of machine learning that uses artificial neural networks with multiple layers to learn complex patterns from enormous amounts of data. Deep learning addresses critical challenges in modern healthcare. This includes physician burnout, diagnostic errors, and healthcare accessibility [7].

The clinical significance extends beyond diagnostic accuracy. Deep learning systems can process vast amounts of medical data in seconds. Furthermore, these technologies have the potential to increase healthcare access by developing expert-level diagnostics.

2. FUNDAMENTALS OF NEURAL NETWORK

Neural networks are a type of machine learning model inspired by the human brain. It consists of interconnected nodes and neurons organized in layers (input, hidden, and output). These neural networks are the foundational technology behind deep learning. Deep learning is also known as deep neural networks, where 'deep' refers to an increased number of layers. This allows the network to learn more complex and abstract features from the data. A basic schematic of neural network architecture is shown in Figure 1.

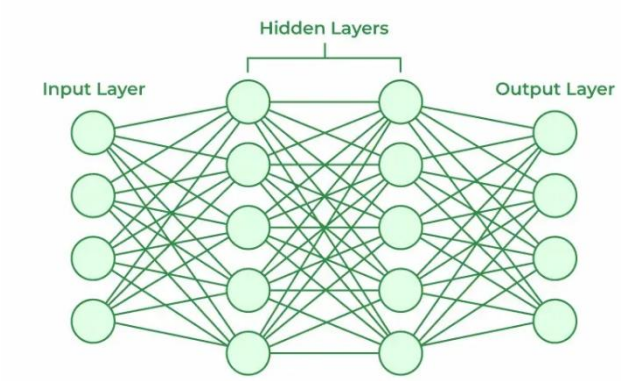

Figure 1: Basic neural network architecture with input, hidden, and output layers. Adapted from [8].

In 1943, neurophysiologist Warren McCulloch and mathematician Walter Pitts introduced the earliest neural network model. They used electrical circuits to represent this network and published their work in a paper titled "A logical calculus of the ideas immanent in nervous activity." However, the first practical implementation was achieved by Frank Rosenblatt, who developed the Perceptron, an early artificial neural network capable of performing pattern recognition.

2.1 Architecture of Artificial Neural Networks

Neural networks are based on the structure and function of the human brain. The fundamental unit of a neural network is an artificial neuron, also called a node, which is a simplified computational model of a biological neuron. Figure 2 is a schematic diagram of a biological neuron in the human brain.

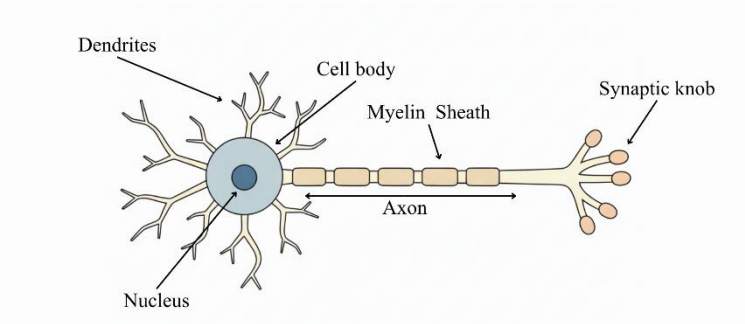

Figure 2: Basic structure of a neuron in the human brain. The schematic illustrates the major components of a typical neuron, including dendrites (which receive signals), the cell body (containing the nucleus), the axon (which transmits an electrical impulse), the myelin sheath (which insulates the axon), and the axon terminals (which form synapses with other neurons or effector cells).

In the context of artificial neural networks, the structure of a biological neuron, illustrated in Figure 2, can be conceptually applied to its computational counterparts. The dendrites correspond to input signals, the cell body and axon together represent the hidden layer, and the synaptic knobs (terminals) are analogous to the output layer.

An artificial neuron receives one or more sets of inputs (x_1, x_2… x_n), also called the input vector. Each of the elements of the input vector is multiplied by a weight (denoted by w) from the weight vector and an addition of a scalar bias (denoted as b). The combined weighted sum (z) can be represented as:

$$z = b + \sum_i w_i x_i \qquad (1)$$

In the last step, the weighted sum is passed through a non-linear function, also known as the activation function. The most common activation functions include sigmoid, tanh, and ReLu (Rectified Linear Unit). The output of the activation function is then passed as input to neurons in the next layer.

The hidden layer is where all the computation occurs. The output layer produces the final prediction as an output vector.

2.2 Convolutional Neural Networks (CNNs)

Convolutional Neural Networks represent the most successful deep learning architecture for medical image analysis. CNNs use three principles: local connectivity, weight sharing, and pooling operations [9]. The CNNs consist of five layers. These are the input layer (or input image), hidden layers (convolutions, pooling, and fully connected), and output layer. Hyperparameters are external configuration variables. These parameters are not based on the data but are set before the training process begins. This controls the model's architecture and learning process.

The convolution layer applies a filter, a small matrix of weights, across an input. This detects features like edges or textures. The layer adds bias at each step to produce an output feature map. Its hyperparameters include filter size F and stride S. A filter size, also known as kernel size, refers to the dimensions of a small matrix that slides over an input image to extract features. Smaller filters capture minute details, while larger filters detect broader patterns. The stride is the number of pixels the filter (or kernel) moves at a time across the input image in each step. The resulting output is a feature map (or activation map), a 2D matrix that highlights specific patterns in the data input.

A pooling layer is a down-sampling operation applied after the convolution layer. It reduces the spatial dimensions (width and height) of the feature map. This results in a decrease in computational load, prevents overfitting, and introduces translation invariance. There are two types of pooling, max and average. The most used pooling is the max pooling. It takes the maximum value within a specified window, preserving the detected features. The average pooling takes the average of the values in the specified window. It down-samples the feature map, losing most delicate details.

The fully connected (FC) layer is the final classification layer. In this layer, each neuron is connected to every neuron in the previous layer. The features extracted by earlier convolutional and pooling layers are flattened into a single vector. This vector is used to perform the final classification or regression task. FC layer performs a linear transformation on the input, which is followed by a non-linear function. If σ Is the activation function, W is the learnable filters or kernels, x is the input layer, and b is the bias, then the output is mathematically represented by equation (2).

$$y = \sigma(Wx + b) \qquad (2)$$

There are three main types of object detection algorithms. Table 1 describes the nature of what is predicted by the object detection algorithms.

Table 1: Object recognition algorithms.

Image Classification	**Classification with localization**	**Detection**
Classifies a picture.	Detects an object in a picture.	Detects up to several objects in a picture.
Predicts probability of object.	Predicts the probability of object and where it is located.	Predicts the probabilities of objects and where they are located.
Traditional CNN	Simplified YOLO, R-CNN	YOLO, R-CNN

Bounding boxes are rectangular regions used in object detection to pinpoint an object's location (as x and y coordinates) within an image. YOLO (You Only Look Once) is a family of real-time object detection systems that predicts bounding boxes and class probabilities simultaneously. R-CNN (Region with Convolutional Neural Network) is an object detection algorithm that performs object detection by not only classifying objects but also localizing them with bounding boxes.

2.3 Recurrent Neural Networks (RNN)

A Recurrent Neural Network (RNN) is designed to recognize the patterns in sequential data. RNNs possess feedback connections, making them suitable for analyzing time-series medical data such as electronic health records (EHRs), patient monitoring signals, and disease progression trajectories [11].

The advantages of RNN include that the model size does not increase with the size of input, considers the historical information, and weights are stored across time. However, it comes with drawbacks such as slow computation, difficulty in accessing information from a long time ago, and the inability to consider future inputs for the current state.

Simple RNNs have a critical limitation known as the 'vanishing gradient problem.' During the training process, the influence of past events can diminish exponentially as the sequence gets longer. This makes it difficult for the network to learn long-range dependencies. For example, an RNN might struggle to connect a diagnosis made years ago to a patient's current symptoms. To solve this problem, RNN variants, LSTM (Long Short-Term Memory) and GRU (Gated Recurrent Units) were developed. These architectures control the flow of information, a mechanism known as the gating mechanism.

2.4 Autoencoders

Autoencoders are a type of neural network used for unsupervised learning. The best use case of this architecture includes dimensionality reduction and feature learning from unlabeled data. In healthcare, autoencoders serve multiple purposes: dimensionality reduction for high-dimensional genomic data, denoising medical images, and learning latent representations of patient phenotypes from EHRs [12]. Figure 3 is an illustration of the Autoencoder architecture.

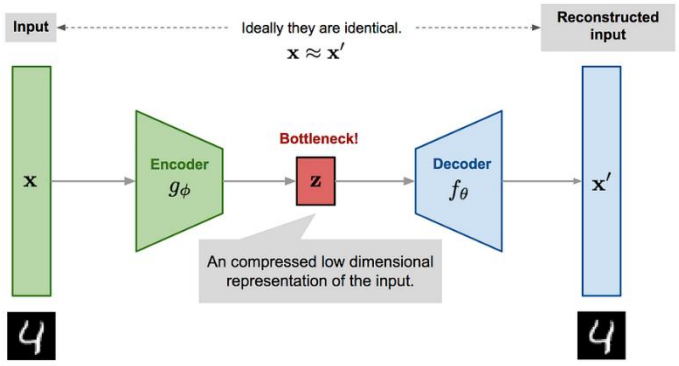

Figure 3: Illustration of the Autoencoder architecture. Source: [13].

Autoencoder architecture consists of the encoder, bottleneck, and decoder. The encoder takes the raw input data and compresses it into a low-dimensional "latent representation." This captures the most salient features of the input, discarding redundant information. The bottleneck (latent space) is the compressed representation of the input data. It is the central layer of the autoencoder. The size of this bottleneck is an important hyperparameter that determines how the data is compressed. The decoder takes the compressed latent representation and reconstructs the original input as accurately as possible.

The autoencoder is trained on an unsupervised learning approach, that is, the training dataset is unlabeled. The reconstruction error is the difference between the original input and the reconstructed output. The autoencoder network is trained to minimize the reconstruction error.

2.5 Transformers

The transformer architecture was first introduced in 2017, initially built for natural language processing, and now increasingly used in fields like healthcare. Transformers are non-recurrent and rely on an attention mechanism. This model consists of an encoder-decoder structure; however, encoder-only (e.g., BERT), decoder-only (e.g., GPT), and encoder-decoder (e.g., T5) variants exist.

The encoder processes the input sequence and generates a representation that captures contextual information. The input tokens are converted into embeddings. Positional encodings are added to these embeddings to preserve the order of tokens. This sequence passes through multiple layers of self-attention and feed-forward networks. The decoder receives embeddings with positional encodings. It then generates output sequences, such as a translated sentence or text, by processing the input and the previously generated tokens.

Self-attention is a mechanism that allows each element in a sequence to relate to and weigh the importance of all other elements in the same sequence. This allows the model to find the most relevant parts of the input sequence. Instead of performing a single attention calculation, the transformer uses multi-head attention. Multiple mechanisms (heads) operate in parallel with the input. This allows the model to capture various relationships in different subspaces of data.

3. APPLICATIONS IN HEALTHCARE

3.1 Medical Imaging

3.1.1 The CheXNet

CheXNet is a dense convolutional neural network (DanseNet). CheXNet was trained on the ChestX-ray14 dataset published in the public repository by the National Institute of Health (NIH). This dataset consists of 112,120 frontal-view X-rays, each labeled for the presence of fourteen different thoracic pathologies, including pneumonia [14].

To evaluate the model's performance, the researchers compared CheXNet to four practicing academic radiologists on a separate test set of 420 images. CheXNet was found to exceed the average radiologist's performance on pneumonia detection. Quantitatively, CheXNet achieved a F1 score of 0.435, which was higher than the radiologist's average of 0.387. The F1 score is the harmonic mean of precision and recall.

However, when CheXNet was evaluated across different hospital systems, certain challenges emerged. A study involving 158,323 chest radiographs from three institutions revealed variable performance. The model trained on one institution's data showed decreased accuracy when assessed on external datasets [15].

This finding highlights the importance of site-specific biases, imaging protocol differences, and population heterogeneity in medical AI deployment.

3.1.2 Breast Cancer Detection

Researchers at Google developed a deep learning system trained on large mammography datasets from over 28,000 women in the UK and the USA. This model was able to identify signs of breast cancer with an accuracy comparable to that of expert radiologists. The AI model produced a significant reduction in both false positives (by 5.7% in the US dataset) and false negatives (by 9.4% in the US dataset) compared to human readers [16].

DeepBreastCancerNet is an example of a novel CNN architecture developed specifically for detecting breast cancer from ultrasound images. It is a 24-layer model incorporating components like inception modules and normalization techniques. It reported a classification accuracy of 99.35% on its test dataset [17].

These findings suggest that if models are trained on an unbiased and normalized dataset, the rate of accuracy increases to a high extent. Creation of AI models based on different modalities (like ultrasound images and mammography) strengthens the ability of these models to adapt to various diagnostic tools.

3.2 Predictive Modeling with Electronic Health Records

3.2.1 BEHRT

BEHRT stands for Bidirectional Encoder Representations from Transformers for Electronic Health Records. It is a deep-learning model based on the transformer architecture (discussed in section 2.5), specifically the encoder-only variant called BERT. BERT is a powerful language model used in natural language processing (NLP) for use with both structured and unstructured medical data.

BEHRT is designed to analyze and predict health conditions from a patient's complete medical history, which is recorded in an Electronic Health Record (EHR). This model learns from complex EHR data by organizing it in a specific way. The encoder creates embeddings that represent a patient's medical history using four types of embeddings: disease, age, visit position, and visit

segment [18]. BEHRT is pre-trained using a masked language model (MLM). MLM allows BEHRT to learn and predict masked (missing) medical concepts within a patient's history. After pre-training, the model can be fine-tuned for a range of tasks, including the prediction of future diagnoses within a certain time frame.

BEHRT is known for its high accuracy compared to previous deep learning models for EHR data. The model can generate patient-specific risk predictions and can be adapted to incorporate different types of data, such as diagnosis, medications, and measurements [19].

3.2.2 StageNet

StageNet is a deep learning model for health risk prediction that uses a stage-aware approach. A stage-aware approach is a method that adapts processing or decision-making based on the current stage or phase within a multi-stage network. StageNet is composed of an LSTM module and a stage-adaptive convolutional module.

The LSTM (Long Short-Term Memory) module is a type of recurrent neural network (discussed in section 2.3). It is designed to learn and remember long-term dependencies in sequence data. A stage-adaptive convolutional module is a neural network component that changes how StageNet processes data depending on which step or stage it's at. This allows StageNet to work better with different types of information [20].

StageNet can provide more accurate health risk predictions and patient subtyping for patients with chronic or progressing diseases. These predictions allow medical professionals to provide treatment plans more effectively.

3.3 Genomics and Drug Discovery

3.3.1 DeepVariant

DeepVariant is a deep-learning-based model developed by Google [21]. This model is used to identify genetic variants inherited from a person's parents. The DeepVariant pipeline takes aligned sequencing data and follows a series of steps to find the genetic variants. The process begins with reading the sequencing data from a BAM or CRAM file format. The model then generates "pileup images." These images are tensors (multi-dimensional arrays) that encode different features of the stacked sequencing reads. Examples include aligning the DNA bases (A, T, C, G), quality scores for the bases, and the DNA strand (forward or reverse).

A trained convolutional neural network (discussed in section 2.2) analyzes the pileup images to classify each genomic locus. It uses statistical patterns to learn and distinguish a true genetic variant from common sequencing errors. The final output is a standard Variant Call Format (VCF) or genomic VCF (gVCF) file. This file lists the identified variants and their genotypes [22].

DeepVariant is recognized for its ability to detect variants that are missed by older, traditional methods, with a lower rate of false positives. It is adaptable for use in non-human species. Major

applications of DeepVariant include whole-genome sequencing (WGS) and whole-exome sequencing (WES). Researchers can train certain DeepVariant models with public data to further improve accuracy, especially for rare variants.

3.3.2 DeepDTA

DeepDTA is a deep learning model developed by Öztürk et al. in 2018. The model predicts the binding affinity between a drug and its target protein using their sequence information. DeepDTA uses two separate blocks of CNN (discussed in section 2.2) to automatically learn high-level feature representations from the one-dimensional sequences of drug and protein.

The model takes two types of input. The first input is the drug's SMILES (Simplified Molecular Input Line Entry System) string, which is a linear text-based representation of a chemical compound. The second input is the raw amino acid (monomer of protein) sequence. The learned representations from the two CNN blocks are then combined and fed into a fully connected layer. This layer predicts a single, continuous numerical value for the binding affinity [23].

The significance of DeepDTA includes its ability to use only the sequences of the compounds and proteins, making it faster and more broadly applicable. However, by relying only on one-dimensional sequences, the model does not consider the three-dimensional structural and spatial relationships that are crucial for protein-ligand interactions.

4. CHALLENGES AND LIMITATIONS

4.1 Data Scarcity

Large deep learning models require millions of parameters, making them notoriously data hungry. A general rule of training these models suggests that training data samples should be at least an order of magnitude greater than the number of model parameters to avoid overfitting. Healthcare is often described as a "big data" field; however, high-quality and well-annotated datasets for specific clinical tasks are often scarce. In cases of rare diseases, the total number of people is finite, making the collection of large datasets a big challenge [24].

4.2 Data Privacy

Patient Health information is among the most sensitive personal data. In the United States of America, the Health Insurance Portability and Accountability Act (HIPAA) establishes national standards to protect sensitive patient health information (PHI) [25]. Patient Privacy regulations, such as HIPAA, create significant barriers to aggregating information from multiple institutions. This results in a data silo problem. A data silo is a problem where data is isolated within a specific department or system. Due to this, most models are trained on data from a single healthcare system.

4.3 Data Quality

In healthcare analytics, the quality of data is often compromised by issues of noise, incompleteness, and heterogeneity. Noise, in this context, refers to the presence of incorrect,

irrelevant, or erroneous information. This often results from imperfect data collection or human error. Incompleteness refers to the lack of key information, partially or completely absent from records. Heterogeneity refers to the variability and fragmentation of data. This is due to varying coding systems used by different institutions (e.g., ID-10, SNOMED CT).

4.4 Black Box Problem

A black box problem is when a system's internal workings are not understandable to humans, even though its inputs and outputs are known. This results in a lack of transparency, making it difficult to trust the system. Due to the inability to understand the reasoning, it is difficult to have confidence in the system's decisions. If the training data contains a bias, it can be hard to identify and correct it, which can lead to unfair outcomes. It is difficult to detect if a black box model has been tampered with through attacks like data poisoning.

4.5 Infrastructure Requirements

Deep learning requires high-end infrastructure. This includes high-performance computing hardware like GPUs (Graphical Processing Units) and TPUs (Tensor Processing Units). These are essential to perform matrix and vector calculations to speed up the training process. Large amounts of Random Access Memory (RAM) are needed to hold large datasets and model parameters. Fast storage, such as solid-state drives (SSDs), is necessary to quickly load data and models into memory. These requirements build up significant costs, making deep learning models very expensive.

5. ADVANCED AI METHODOLOGIES

5.1 Explainable AI (XAI)

Explainable AI, also known as XAI, is a set of processes that make AI decision-making understandable to humans. XAI provides transparency and accountability, which allows users to understand why an AI model makes a specific decision. XAI techniques are useful to solve the black box problem (discussed in section 4.4) as they give the ability to build trust, debug errors, and identify biases.

5.1.1 Local Interpretable Model-Agnostic Explanations (LIME)

LIME (Local Interpretable Model-Agnostic Explanations) is an XAI method that explains the predictions of any deep learning model. It explains a specific, individual prediction (data instance) and does not explain the model's behavior globally across all data. The explanations provided are simple and easy for a human to understand. LIME can be applied to any deep learning model, regardless of its underlying architecture or complexity.

5.1.2 SHapley Additive exPlanations (SHAP)

SHAP (SHapley Additive exPlanations) is a framework that uses game theory to explain the output of any deep learning model. SHAP is known for its fairness and theoretical consistency. It can be

used for a wide variety of applications, like interpreting risk factors in healthcare. SHAP is more expensive than LIME; however, its consistency makes it a preferred method for high-stakes applications, including brain tumor detection and diabetes prediction.

5.1.3 Gradient-weighted Class Activation Mapping (Grad-CAM)

Grad-CAM is a technique that creates a visual explanation, or a "heat map," for deep neural network decisions. It works by highlighting which parts of an image were most important for the model to make a specific classification. This helps to make the model more interpretable. It can help identify when a model is focusing on the wrong features. Some applications of Grad-CAM include its use in medical imaging to highlight relevant areas in an X-ray diagnosis.

5.2 Graph Neural Networks (GNN)

GNNs (Graph Neural Networks) are a type of artificial neural network that is designed to work with data structured as graphs. It consists of nodes and edges that represent relationships. GNNs are used for patient relationship modeling and risk prediction. This is done by representing patients and their relationships as graphs. This approach can extract patterns from electronic health records (EHRs), identify correlated diagnoses, and cluster similar patients. This can lead to more accurate risk predictions for conditions like cardiovascular diseases or Alzheimer's.

6. EVALUATION AND VALIDATION

Accuracy is a fundamental metric in deep learning models. Evaluation and validation metrics are used to assess the accuracy and performance of a model on unseen data. Evaluation metrics are specific calculations used to score a model's performance. Validation techniques are methods used to systematically evaluate the model and prevent issues like overfitting.

6.1 Sensitivity

Sensitivity, also known as recall or true positive rate, is a model evaluation metric that measures the proportion of actual positive cases that the model correctly identifies. Sensitivity is crucial in situations where missing a positive case has significant consequences, such as a medical diagnosis to detect a disease. A high sensitivity means the model is good at identifying all the positive cases. The formula for sensitivity is given by:

$$Sensitivity = \frac{True\ Positives}{True\ Positives + False\ Negatives} \qquad (3)$$

6.2 Specificity

Specificity, also known as the true negative rate, is a validation metric that measures a model's ability to correctly identify actual negative cases. A high specificity indicates that the model is good at avoiding false positives and correctly classifying negative instances. It is crucial in high-stakes applications like medical diagnostics. It is often evaluated alongside sensitivity (section 6.1)

to provide a more complete picture of the model's performance than accuracy alone. The formula of specificity is given by:

$$Specificity = \frac{True\ Negatives}{True\ Positives + False\ Negatives} \qquad (4)$$

6.3 Precision

Precision measures the accuracy of positive predictions, calculated as the number of true positives divided by the total number of positive predictions. A higher precision score indicates that fewer false positives were generated. The formula for precision is given by:

$$Precision = \frac{True\ Positives}{True\ Positives + False\ Positive} \qquad (5)$$

6.4 F1 Score

The F1 score is a metric used to evaluate a model's performance in classification tasks by balancing two other metrics: precision and recall (sensitivity). It is calculated as the harmonic mean of precision and recall. A higher F1 score indicates better performance, with a perfect score being 1. The formula for the F1 score is given by:

$$F1 = 2 \times \frac{Precision \times Recall}{Precision + Recall} \qquad (6)$$

6.5 Mean Absolute Error (MAE)

Mean Absolute Error (MAE) is a metric used to measure the average magnitude of errors between the predicted and actual values. It is calculated as the average of the absolute differences between the predicted and actual values. The formula for MAE is given by:

$$MAE = \frac{1}{n}\sum_{i=1}^{n}|y_i - \hat{y}_i| \qquad (7)$$

In equation (7), n is the number of data points, y_i is the actual value, and $\hat{y}_i$ is the predicted value for the i^{th} data point.

6.6 Mean Squared Error (MSE)

Mean Squared Error (MSE) is a common loss function that measures the average of the squares of the errors between predicted and actual values. It quantifies how close a model's predictions are to the true values. A lower MSE indicates a more accurate model. The formula for MSE is given by:

$$MSE = \frac{1}{n}\sum_{i=1}^{n}(\hat{y}_i - y_i)^2 \qquad (8)$$

In equation (8), n is the number of data points, $\hat{y}_i$ is the predicted value, and y_i is the actual value for the i^{th} data point.

6.7 Root Mean Squared Error (RMSE)

Root Mean Squared Error (RMSE) is a metric to measure the difference between predicted and actual values. This is done by finding the square root of the average of the squared errors. A lower RMSE indicates a better-trained model. The formula for RMSE is given by:

$$RMSE = \sqrt{\frac{1}{n}\sum_{i=1}^{n}(f_i - o_i)^2} \qquad (9)$$

In equation (9), n is the number of data points, f_i is the predicted value for the i^{th} observation, and o_i is the actual value for the i^{th} observation.

6.8 Mean Average Precision (mAP)

Mean Average Precision (mAP) is an evaluation metric in tasks like object detection. It considers both precision and recall (sensitivity). mAP evaluates both how well the model identifies the object (classification) and how accurately it localizes it with a bounding box (localization). The formula for mAP is given by:

$$mAP = \frac{1}{n}\sum_{i=1}^{n} AP_i \qquad (10)$$

In equation (10), n is the number of classes and AP_i is the average precision for the i^{th} class. Average Precision is calculated as the area under the precision-recall curve.

6.9 Intersection over Union (IoU)

Intersection over Union (IoU) is an evaluation metric used to quantify the localization accuracy of a model's prediction compared to the actual target. Localization accuracy is the measure of how precisely a model can determine the spatial location of an object in an image. IoU is also known as the Jaccard Index or Jaccard similarity coefficient. A ground-truth region is the labeled coordinates that represent the actual location and extent of an object in the data. IoU is defined as the ratio of the area of overlap (intersection) between the predicted and ground-truth regions to the total combined area (union) of both regions.

7. CASE STUDY – GOOGLE'S LYNA

Google's LYNA stands for Lymph Node Assistant, a deep learning model that helps pathologists detect breast cancer that has spread to the lymph nodes. LYNA was developed by Google AI and researchers at the Naval Medical Center San Diego. Studies indicate that pathologists working with LYNA assistance can achieve higher accuracy than AI or a human alone [26].

7.1 The Clinical Problem

Pathologists sometimes miss small clusters of cancer cells (micro metastases) in lymph node tissue. Studies cited by Google showed that the sensitivity of detecting small metastases on individual slides could be as low as 38% for pathologists under time constraints [27]. The average time for a pathologist to review a single slide without AI assistance was around two minutes.

There was a need for a tool to improve the consistency and diagnostic accuracy of pathologists. This would address the concern of accuracy, crucial for a patient's prognosis and treatment planning. Metastases are responsible for the majority (around 90%) of breast cancer-related deaths.

7.2 Dataset Used

The development of LYNA was based on a publicly available and de-identified dataset. A de-identified dataset has its personally identifiable information (PII) removed or altered so that individuals cannot be identified. It was trained and tested on two datasets.

The first dataset was the Cemelyon16 Dataset. This dataset was compiled for the "Cancer Metastases in Lymph Nodes 2016" challenge and provided by the Radboud University Medical Center and University Medical Center Utrecht, both in the Netherlands. This dataset consists of 399 whole-slide images (WSIs) of hematoxylin-eosin-stained lymph node sections from breast cancer patients [28]. 277 slides were used for training the LYNA algorithm, and the remaining 129 slides were used as an evaluation set to test the model's performance.

The second dataset was provided by co-authors at the Naval Medical Center San Diego. It includes an additional 108 images from 20 patients. The researchers used this dataset to test the algorithm's robustness to image variability.

7.3 Model Architecture

The foundation of LYNA is the Inception-v3 architecture, which is a convolutional neural network (CNN). It is known for its efficiency and high accuracy in general image recognition tasks. The model takes as input a 299-pixel by 299-pixel image. However, the original Inception-v3 model was modified for this specific application. LYNA was designed to examine images at different magnifications, like how a pathologist reviews slides. The training process was made more computationally efficient. This allowed the algorithm to "see" a greater diversity of tissue samples.

7.4 Performance and Results

LYNA achieved approximately 99% accuracy in correctly distinguishing slides with metastatic cancer from those without, even when the regions were very small. The model achieved a 91% tumor-level sensitivity. This made this algorithm highly effective at pinpointing the exact location of cancer and other suspicious regions within a slide. At a very sensitive threshold, the model achieved 69% sensitivity, identifying all 40 metastases in one evaluation dataset with no false

positives. LYNA was unaffected by common slide artifacts like air bubbles, poor staining, or over-fixation [29].

When pathologists used LYNA's assistance, their average slide review time was cut in half. Pathologists working with LYNA were more accurate than either the algorithm alone or unassisted pathologists. They reported that LYNA made the laborious task of detecting small metastases subjectively easier.

8. Conclusion

This research paper provided an in-depth study of deep learning methodologies and their technical applications in healthcare. Deep learning has become one of the most transformative technologies in the healthcare sector, surpassing traditional diagnostic and prognostic approaches. The study emphasized the growing reliance on deep learning owing to its abilities in feature extraction, pattern recognition, and decision-making.

The fundamentals of neural networks were examined, establishing a theoretical foundation for their use in medicine. Architectures such as Convolutional Neural Networks (CNNs), Recurrent Neural Networks (RNNs), Autoencoders, and Transformers were analyzed for how they work and their suitability for specific healthcare tasks. CNNs demonstrated high performance in processing spatial data, with successful applications like Google LYNA. RNNs and Transformers proved crucial in modeling sequential data such as patient histories and electronic health records (EHRs).

In medical imaging, models like CheXNet and LYNA achieved expert-level accuracy in detecting thoracic diseases and metastatic breast cancer, respectively. Architectures like BEHRT and StageNet utilized EHRs to predict disease progression accurately. In genomics and drug discovery, models such as DeepVariant and DeepDTA exemplify how deep neural networks can classify genetic variants and predict molecular interactions.

Despite these advancements, significant challenges still exist. Issues such as data scarcity, privacy concerns, data quality, and the black box problem hinder clinical adoption. Additionally, computational and infrastructure demands create barriers to developing efficient deep learning models. To overcome these issues, explainable AI (XAI) and Graph Neural Networks (GNN) offer promising solutions for more interpretable and context-aware models.

The evaluation metrics discussed include sensitivity, specificity, and F1 score, which are essential for assessing a model's reliability and guiding further improvements. Overall, deep learning holds great promise for advancing healthcare. Achieving this requires interdisciplinary collaboration to address technical, ethical, and logistical challenges.

In conclusion, while deep learning offers substantial benefits, future research should focus on making these systems transparent and scalable, and on integrating them responsibly into healthcare settings to maximize patient benefits.

REFERENCES

[1] D. Crevier, *AI: The Tumultuous Search for Artificial Intelligence,* New York, NY, USA: BasicBooks, 1993.

[2] H. P. Newquist, *The Brain Makers: Genius, Ego, and Greed in the Quest for Machines That Think*, New York, NY, USA: Macmillan/SAMS, 1994, pp. 92–98.

[3] E. Shortliffe, Ed., *Computer-based medical consultations: MYCIN*, vol. 2, Elsevier, 2012.

[4] Y. LeCun, Y. Bengio, and G. Hinton, "Deep Learning," *Nature*, vol. 521, no. 7553, pp. 436-444, 2015.

[5] A. Krizhevsky, I. Sutskever, and G. E. Hinton, "ImageNet classification with deep convolutional neural networks," in *Proc. NIPS*, 2012, pp. 1097-1105.

[6] A. Esteva et al., "Deep learning-enabled medical computer vision," *NPJ Digital Med.*, vol. 4, no. 1, pp. 1-9, 2021.

[7] E. J. Topol, "High-performance medicine: the convergence of human and artificial intelligence," *Nature Med.*, vol. 25, no. 1, pp. 44-56, 2019.

[8] GeeksforGeeks, “What is a Neural Network?” GREEKSFORGREEKS.com. Accessed: Oct. 14, 2025. [Online.] Available: https://www.geeksforgeeks.org/machine-learning/neural-networks-a-beginners-guide

[9] Y. LeCun, L. Bottou, Y. Bengio, and P. Haffner, "Gradient-based learning applied to document recognition," *Proc. IEEE*, vol. 86, no. 11, pp. 2278-2324, Nov. 2002.

[10] A. Amidi and S. Amidi. (2019). CS 230 – Deep Learning [Online]. Available: https://stanford.edu/~shervine/teaching/cs-230

[11] Z. C. Lipton, D. C. Kale, C. Elkan, and R. Wetzel, "Learning to diagnose with LSTM recurrent neural networks," in *Proc. Int. Conf. Learn. Representations (ICLR)*, 2016. [Online]. Available: https://arxiv.org/abs/1511.03677

[12] R. Miotto et al., "Deep patient: An unsupervised representation to predict the future of patients from the electronic health records," *Sci. Rep.*, vol. 6, Art. no. 26094, 2016.

[13] V. E. Irekponor, “Mathematical Prerequisites for Understanding Autoencoders and Variational Autoencoders (VAEs): Beginner Friendly, Intermediate Exciting, and Expert Refreshing,” *Medium*, May 28, 2020. [Online]. Available: https://medium.com/analytics-vidhya/mathematical-prerequisites-for-understanding-autoencoders-and-variational-autoencoders-vaes-8f854025390e

[14] P. Rajpurkar et al., "CheXNet: Radiologist-level pneumonia detection on chest X-rays with deep learning," *arXiv preprint* arXiv:1711.05225, 2017.

[15] J. R. Zech et al., "Variable generalization performance of a deep learning model to detect pneumonia in chest radiographs: A cross-sectional study," *PLOS Med.*, vol. 15, no. 11, pp. 1–17, Nov. 2018.

[16] S. M. McKinney *et al*., “International evaluation of an AI system for breast cancer screening,” *Nature*, vol. 577, pp. 89-94, 2020.

[17] A. Raza, N. Ullah, J. A. Khan, M. Assam, A. Guzzo, and H. Aljuaid, "DeepBreastCancerNet: A novel deep learning model for breast cancer detection using ultrasound images," *Appl. Sci.*, vol. 13, no. 4, Art. no. 2082, 2023.

[18] Y. Li, S. Rao, J. R. A. Solares, A. Hassaine, R. Ramakrishnan, D. Canoy, Y. Zhu, K. Rahimi, and G. Salimi-Khorshidi, "BEHRT: Transformer for electronic health records," *Sci. Rep.*, vol. 10, no. 1, p. 7155, 2020.

[19] J. Wang *et al*., "Recent advances in predictive modeling with electronic health records," in *Proceedings of the International Joint Conference on Artificial Intelligence (IJCAI)*, vol. 2024, p. 8272, August 2024.

[20] J. Gao, C. Xiao, Y. Wang, W. Tang, L. M. Glass, and J. Sun, "StageNet: Stage-aware neural networks for health risk prediction," in *Proceedings of the Web Conference 2020*, Apr. 2020, pp. 530-540.

[21] Google, "DeepVariant," GitHub repository, 2025. [Online]. Available: https://github.com/google/deepvariant. [Accessed: Oct. 15, 2025].

[22] NVIDIA, "DeepVariant," in *NVIDIA Clara Parabricks Documentation*. [Online]. Available: https://docs.nvidia.com/clara/parabricks/latest/documentation/tooldocs/man_deepvariant.html. [Accessed: Oct. 15, 2025].

[23] H. Öztürk, A. Özgür, and E. Ozkirimli, "DeepDTA: deep drug–target binding affinity prediction," *Bioinformatics*, vol. 34, no. 17, pp. i821–i829, 2018.

[24] L. Alzubaidi *et al.*, "A survey on deep learning tools dealing with data scarcity: definitions, challenges, solutions, tips, and applications," *J. Big Data*, vol. 10, no. 1, p. 46, 2023.

[25] P. F. Edemekong *et al.*, “Health Insurance Portability and Accountability Act (HIPAA) Compliance,” *StatPearls [Internet]*, Treasure Island (FL): StatPearls Publishing, Nov. 24, 2024. Available: https://www.ncbi.nlm.nih.gov/books/NBK500019.

[26] D. F. Steiner *et al.*, “Impact of deep learning assistance on the histopathologic review of lymph nodes for metastatic breast cancer,” *Am. J. Surg. Pathol.*, vol. 42, no. 12, pp. 1636–1646, 2018.

[27] M. Stumpe and L. Peng, “Assisting pathologists in detecting cancer with deep learning,” *Google AI Blog*, pp. 1–11, 2017.

[28] J. Stone, “Studies show potential for Google’s AI tools to improve pathologist accuracy and efficiency,” *Dark Daily*, Nov. 5, 2018. [Online]. Available: https://www.darkdaily.com/2018/11/05/studies-show-potential-for-googles-ai-tools-to-improve-pathologist-accuracy-and-efficiency. [Accessed: Nov. 6, 2025].

[29] S. Bhattacharya *et al.*, “Empowering precision medicine: regenerative AI in breast cancer,” *Front. Oncol.*, vol. 14, art. no. 1465720, 2024.